

Virtual Pulmonary Valve Replacement Interventions with a Personalised Cardiac Electromechanical Model

Tommaso Mansi¹, Barbara André², Michael Lynch³, Maxime Sermesant⁴, Hervé Delingette⁵, Younes Boudjemline⁶ and Nicholas Ayache⁷

Abstract Pulmonary valve replacement (PVR) is a pivotal treatment for patients who suffer from chronic pulmonary valve regurgitations. Two PVR techniques are becoming prevalent: a minimally invasive approach and an open-heart surgery with direct right ventricle volume reduction. However, there is no common agreement about the postoperative outcomes of these PVR techniques and choosing the right therapy for a specific patient remains a clinical challenge. We explore in this paper how image processing algorithms, electromechanical models of the heart and real-time surgical simulation platforms can be adapted and combined together to perform patient-specific simulations of these two PVR therapies. We propose a framework where 1) an electromechanical model of the heart is personalised from clinical MR images and used to simulate the effects of PVR upon the cardiac function; 2) volume reduction surgery is simulated in real-time by interactively cutting, moving and joining parts of the anatomical model. The framework is tested on a young patient. The results are promising and suggest that such advanced biomedical technologies may help in decision support and surgery planning for PVR.

¹ Asclepios, INRIA-Sophia-Méditerranée, Sophia-Antipolis, France
tommaso.mansi@sophia.inria.fr

² Asclepios, INRIA-Sophia-Méditerranée, Sophia-Antipolis, France
barbara.andre@sophia.inria.fr
Mauna Kea Technologies, Paris, France
barbara.andre@maunakeatech.com

³ Siemens AG, CT SE SCR2, Erlangen, Germany

⁴ Asclepios, INRIA-Sophia-Méditerranée, Sophia-Antipolis, France
maxime.sermesant@sophia.inria.fr

⁵ Asclepios, INRIA-Sophia-Méditerranée, Sophia-Antipolis, France
herve.delingette@sophia.inria.fr

⁶ Service de Cardiologie Pédiatrique, Hôpital Necker Enfants Malades, Paris, France
younes.boudjemline@nck.ap-hop-paris.fr

⁷ Asclepios, INRIA-Sophia-Méditerranée, Sophia-Antipolis, France
nicholas.ayache@sophia.inria.fr

Introduction

Pulmonary valve replacement (PVR) is a pivotal treatment for patients who suffer from chronic pulmonary valve regurgitations. Two PVR techniques are becoming prevalent. On the one hand, percutaneous PVR (PPVR) aims at inserting new pulmonary valves using minimally invasive methods [11]. However, this technique is only possible if the diameter of the right ventricle (RV) outflow tract is lower than 22 mm. On the other hand, a recent surgical approach consists in replacing the pulmonary valves and directly remodelling the RV [16]. The surgeon not only replaces the valves but also intentionally resects the regions of the RV myocardium that are impaired by fibrosis or scars, to reduce RV volume and improve its function. However, there is no common agreement about the postoperative effects of these techniques upon the RV function, which most probably depend on patient pathophysiology. Choosing the appropriate therapy for a given patient remains a clinical challenge.

In this paper, we explore how a fast computational model of ventricular electromechanics can be combined with image processing algorithms and an interactive surgical simulation platform to simulate the direct postoperative effects of these two PVR therapies. In the last decade, several electromechanical (EM) models of the heart have been proposed to simulate the phenomena that govern the cardiac activity, from electrophysiology to biomechanics [8, 13, 18]. Primarily developed for the understanding of the organ, recent research now aims at applying them in patient-specific simulations [18, 24]. At the same time, platforms for virtual soft-tissue interventions are becoming efficient enough to allow the real-time simulation of complex surgical interventions [4]. In Tang et al. [21], the authors proposed a first promising approach for patient-specific virtual PVR and RV volume reduction surgery. In their study, they made use of an advanced fluid-structure interaction model and considered the myocardium as a passive isotropic tissue. However, although they obtained satisfying results, they did not simulate the preoperative regurgitations and the active properties of the myocardium.

We propose in this study to use an active anisotropic EM model of the heart, with a simple model of regurgitations. As in [18, 21], we aim at controlling the model with clinically related data. Hence, some simplifications in the model are made while still capturing the main features of the cardiac function.

Fig. 1 shows the different elements of the proposed framework, made as modular as possible to allow seamless integration of advanced and specific tools. The biventricular myocardium is semi-automatically segmented from clinical 4D cine MRI, excluding the papillary muscles. The mesh obtained from the time frame at mid-diastole is used as 3D anatomical model to simulate patient cardiac function and PVR therapies. The variation of the blood pool volumes throughout the cardiac cycle is computed to calibrate the EM model. After calibration, the EM model is used to simulate the patient cardiac functions. To simulate the replacement of the valves, regurgitations are disabled. Virtual RV volume reduction sur-

gery is interactively performed on the mesh, in real-time, using SOFA [3], an open source soft-tissue intervention platform.

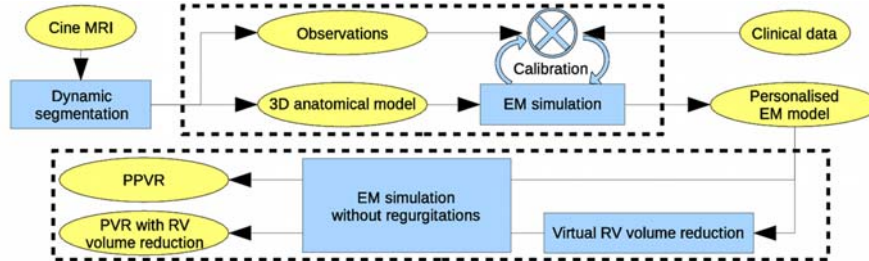


Fig. 1. Pipeline for model-based simulation of PVR therapies (*see details in text*).

Methods

Anatomical Model

The first step of the framework consists in creating a 3D anatomical model of the patient biventricular myocardium. This model is made up of two main elements, the geometry of the myocardium and the orientation of the myofibres.

Myocardium Geometry

Countless segmentation techniques are available in the literature, often based on prior knowledge [9, 12]. However, because patients with serious pulmonary valve regurgitations present extreme variability in heart anatomy, such methods are unsuitable for our purposes. We thus decided to combine specific image processing techniques to efficiently extract the biventricular myocardium from the cine MRI.

First, the left ventricle (LV) endocardium and the epicardium are delineated on the first frame of the MRI cardiac sequence by using an interactive tool based on variational implicit functions [22]. The user places control points inside, on and outside the desired surface. The algorithm computes in real-time the implicit function that interpolates those points and extracts its 0-level set (see Fig. 2). The resulting surface is tracked throughout the cardiac cycle using a diffeomorphic non-linear registration method [23].

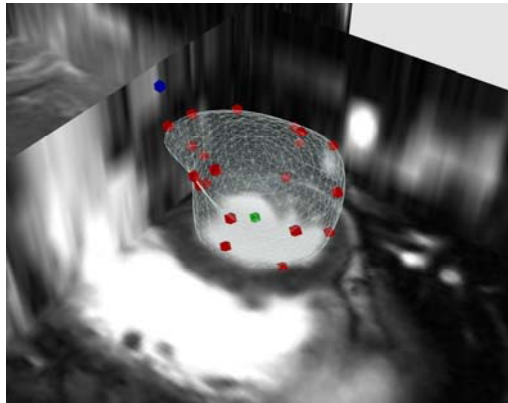


Fig. 2. Interactive segmentation of the left ventricle. The 3D surface (*wireframe*) is interactively modelled by placing surface landmarks (*red points*), inside landmarks (*green point*) and outside landmarks (*blue point*). The algorithm automatically updates the underlying implicit function and extracts the 0-level set surface.

Second, because segmenting the RV in patients with chronic pulmonary valve regurgitations is more challenging than segmenting the LV due to extreme variability in shape and reduced image contrast, the RV endocardium is segmented on all the frames of the cardiac sequence by fitting an anatomically accurate geometrical model. Its position, orientation and scale in the images are determined using minimal user interaction. Boundaries are locally adjusted by training a probabilistic boosting tree classifier with steerable features [25]. The resulting RV endocardium is tracked throughout the cardiac cycle using an optical flow method.

Finally, the binary masks of the segmented epicardium and endocardia are combined together to get a dynamic mask of the biventricular myocardium. The valve plane is manually defined and muscle consistency is ensured by preserving a minimal thickness of 3 mm (mean thickness of a healthy RV myocardium). Dynamic 3D surfaces are computed using CGAL library [1] and simplex-based deformable surfaces [14]. The surface mesh at the mid diastole time frame is finally transformed into a tetrahedral volume mesh using GHS3D [2] (see Fig. 3).

Myocardium Fibres

Next, the orientations of the myocardium fibres are defined. As their *in-vivo* measurement is still an open challenge, we use a computational model based on observations on anatomical dissections or post-mortem diffusion tensor images. These studies showed that fibre orientation varies from -70° on the epicardium to 0° at mid-wall to $+70^\circ$ on the endocardium [6]. Synthetic fibres are thus created by linearly interpolating their orientation with respect to the short axis plane, from -90° on the epicardium to 0° at mid-wall to $+90^\circ$ on the endocardium. Angles are

over-estimated to account for averaging, one fibre orientation being associated to one tetrahedron.

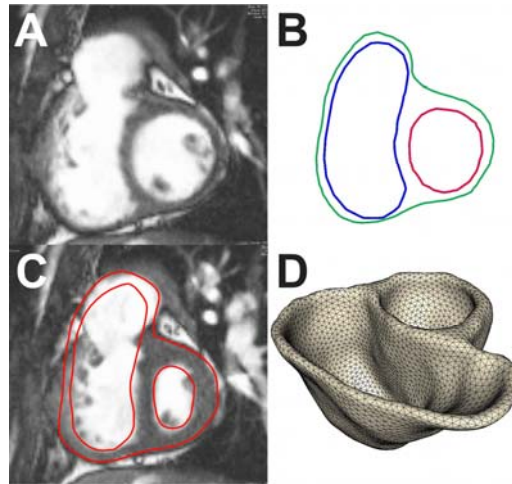


Fig. 2. Cine MRI segmentation. a-b) Image and contours at end-diastole: epicardium (*green*), LV (*red*) and RV (*blue*). c) Tracked myocardium contour at end-systole (*red*). d) 3D mesh of the biventricular myocardium.

Electromechanical Model

Once the volumetric anatomical model is built, computational models of myocardium electrophysiology and biomechanics can be applied on it. Different boundary conditions enable the modelling of the four cardiac phases and the orientation of the myocardium fibres is considered to cope with myocardium anisotropy. For the sake of interactivity, fast algorithms based on finite element method (FEM) are used in this study. Furthermore, because we aim at controlling the model with clinical data, simplifications are introduced while still capturing the main features of the pathological cardiac function.

Electrophysiology

The Eikonal approach [10] detailed in [19] is used to model electrophysiology. This method is computationally efficient and has shown good results when simulating the propagation of the electrical wave in healthy subjects and in patients with no apparent wave re-entry [10,19], such as in the early stages of the patholo-

gies we are interested in. Essentially, the depolarisation time T_d of the electrical wave is computed at each vertex of the volume mesh by solving the anisotropic Eikonal equation $v^2(\nabla T_d^t D \nabla T_d) = 1$. In this equation, v is the local conduction velocity and D the tensor defining the conduction anisotropy. In the fibre orientation \mathbf{f} coordinates, D writes $D = \text{diag}(1, \rho, \rho)$, where ρ is the conduction anisotropy ratio between longitudinal and transverse directions.

Biomechanics

Biomechanics are simulated by using the FEM model proposed by Bestel-Clement-Sorine [7], later simplified in [18]. Despite its relative simplicity with respect to other more comprehensive models [8,13], this model is able to simulate the main features of cardiac motion as observed in images of healthy subjects and patients with less severe diseases [18]. It is controlled by a few clinically related parameters and is fast enough to allow personalisation from clinical data.

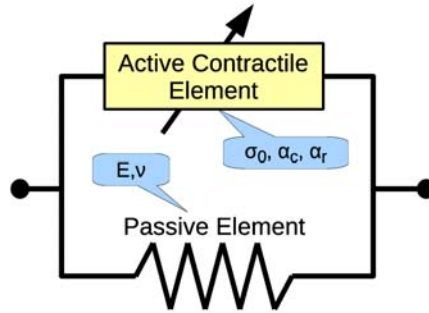


Fig. 3. Scheme of the biomechanical model with related parameters (*see details in text*).

The constitutive law is composed of two elements (see Fig. 4). A passive element models the properties of the myocardium tissue. We use linear anisotropic visco-elasticity, controlled by the Young modulus E and the Poisson ratio ν . The second element is an active contractile element, which is controlled by the depolarisation time T_d computed with the Eikonal equation. It generates an anisotropic contraction tensor $\Sigma(t) = \sigma_c(t) \cdot \mathbf{f} \otimes \mathbf{f}$ which results in a contraction force \mathbf{f}_c on each vertex. Σ depends on the time t , the fibre orientation \mathbf{f} and the strength of the contraction $\sigma_c(t)$ as defined by equation (1):

$$\begin{cases} \text{if } T_d \leq t \leq T_r : \sigma_c(t) = \sigma_0(1 - \exp(\alpha_c(T_d - t))) \\ \text{if } T_r < t < T_d + \text{HP} : \sigma_c(t) = \sigma_c(T_r)(\exp(\alpha_r(T_r - t))) \end{cases} \quad (1)$$

where $T_r = T_d + \text{APD}$ is the repolarisation time, APD the action potential duration, HP the heart period, σ_0 the maximum active contraction and α_c and α_r the contraction and relaxation rates respectively.

Boundary Conditions and Pulmonary Valve Regurgitations

The four phases of the cardiac cycle - filling, isovolumetric contraction, ejection and isovolumetric relaxation - are simulated as detailed in [18]. During ejection (respectively filling), a pressure constraint equal to the arterial (resp. atrial) pressure is applied to the endocardia. Flows are obtained as the variations of the blood pool volumes. A 3-element Windkessel model [20] is employed to simulate the arterial pressures. During the isovolumetric phases, a penalty constraint is applied to the endocardia to keep the cavity volumes constant. Then, when the ventricular pressure becomes higher (resp. lower) than the arterial (resp. atrial) pressure, ejection (resp. filling) starts.

In this study we are interested in the global effects of the regurgitations on the RV function. Because of the absence of pulmonary valves, blood can always flow between the RV and the pulmonary artery. However, in our implementation of the cardiac phases, regurgitations affect the RV isovolumetric phases only, when the volume can vary due to the regurgitations. If the regurgitation flows ϕ_c and ϕ_r at contraction and relaxation respectively are known, by means of echocardiography for instance, we can modify the isovolumetric phases as follows. At each instant t , we first estimate the volume variation ΔV , during Δt , that we would have if the myocardium was free from isovolumetric constraint. Then:

- if $|\Delta V| > |\phi_{\{c,r\}} * \Delta t|$, a penalty constraint is applied to each vertex of the RV endocardium such that the resulting volume variation becomes $\Delta V = \phi_{\{c,r\}} * \Delta t$. The effect of the active force \mathbf{f}_c is thus partially compensated.
- Otherwise, no penalty constraint is applied: \mathbf{f}_c is not counterbalanced.

In this way, the blood pool volume can change during the isovolumetric phases according to the measured regurgitation flows.

Real-Time Simulation of Soft-Tissue Interventions

The last component of the proposed pipeline aims at simulating the RV volume reduction surgery. This task is implemented in SOFA, an open source soft-tissue intervention platform [3]. Interactively, the user remodels the heart geometry by resecting any region of the RV myocardium and closing the remaining wall to recreate the cavity. To cope with large displacements and rotations of the elements, the myocardium biomechanics are simulated using a corotational FEM model [15]. An implicit solver is used to update the mesh position.

Tissue Resection

Tissue resection is performed in two steps. First, a sphere of interest is defined in the SOFA scene by picking two elements of the myocardium surface that define the centre and the radius. Next, all the elements of the mesh laying within this sphere of interest and that are connected to the central element are removed. To this aim, the method proposed by André et al. [5], available in the SOFA platform, is used. To ensure interactivity and real-time execution, the authors store all the indices of the mesh elements and all the information attached to them into arrays with contiguous memory storage and short access time. In this way, when the mesh is locally modified, the time to update the data structures does not depend on the total number of mesh elements but only on the number of modified elements. On the other hand, this also implies element renumbering to keep the arrays contiguous in case of element removal, but this procedure is transparent to the user and does not affect the interactivity in our application. Through iterative selection of central elements and radius sizes, the myocardium tissue can be resected as desired (Fig. 5, left panel).

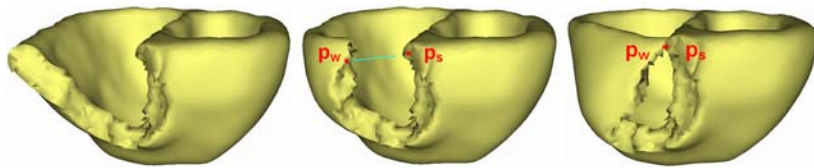


Fig. 4. Virtual suture of the RV. Each side of the resected area (*left panel*) is brought close to each other (*mid panel*). Then, two vertices p_w and p_s are picked up and p_w position is constrained to coincide with p_s , deforming the RV free wall accordingly (*right panel*).

Tissue Attachment

After resection, the RV is interactively and carefully reconstructed without deforming the LV. The boundaries of the resected area are interactively drawn close to each other (Fig. 6). Next, a vertex on one side of the resected area is picked up and fixed to a second vertex on the other side (Fig. 5, mid panel). As a result, the RV morphology globally deforms until reaching a minimal energy state. As this procedure can create holes and generate a chaotic mesh topology in the junction, the deformed geometry is remeshed after rasterisation as a binary image.

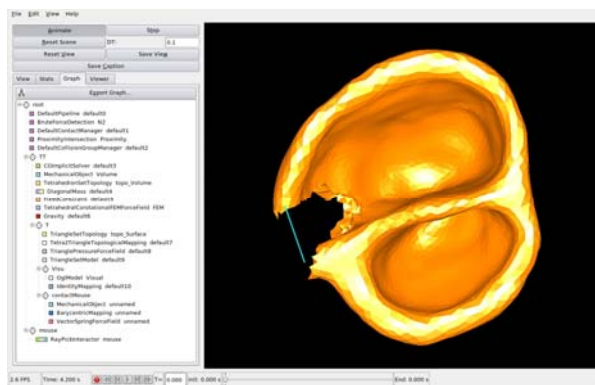


Fig. 5. Screenshot of the SOFA platform. The user is remodelling the geometrical model of a heart. After resection, the user is closing the free-wall by pulling it close to the septum (blue line).

Myocardium Fibres Recovery

As fibre orientations are intrinsic to the elements of the tetrahedral mesh, they must be preserved during the virtual intervention. Fibres are mapped from the original model to the deformed geometry using local barycentric coordinate systems, preserving in this way their relative orientation in the tetrahedron coordinate system. Then, the resulting fibre orientations are transferred to the final remeshed model by using an intermediate rasterisation of the fibre directions as a vector image.

Experiment and Results

The framework is tested on a randomly selected patient (age=17) with repaired Tetralogy of Fallot, a severe congenital heart disease that requires surgical repair

in infancy. The clinical evaluation of this patient showed chronic pulmonary valve regurgitations, an extremely dilated RV and an abnormal motion of the RV outflow tract. LV and RV functions were normal as well as electrophysiology. RV pressure at end-systole was about 50 mmHg (estimated using echocardiography). To date, this patient has undergone no PVR therapy.

Magnetic resonance imaging was performed using 1.5T MR scanner (Avanto, Siemens Medical Systems, Erlangen, Germany). Retrospective gated steady-state free precession (SSFP) cine MRI of the heart were acquired in the short-axis view covering the entirety of both ventricles (10 slices; slice thickness, 8 mm; temporal resolution, 25 frames). Images were made isotropic (1x1x1mm) and contrast was enhanced by clamping the tails of the grey-level histogram.

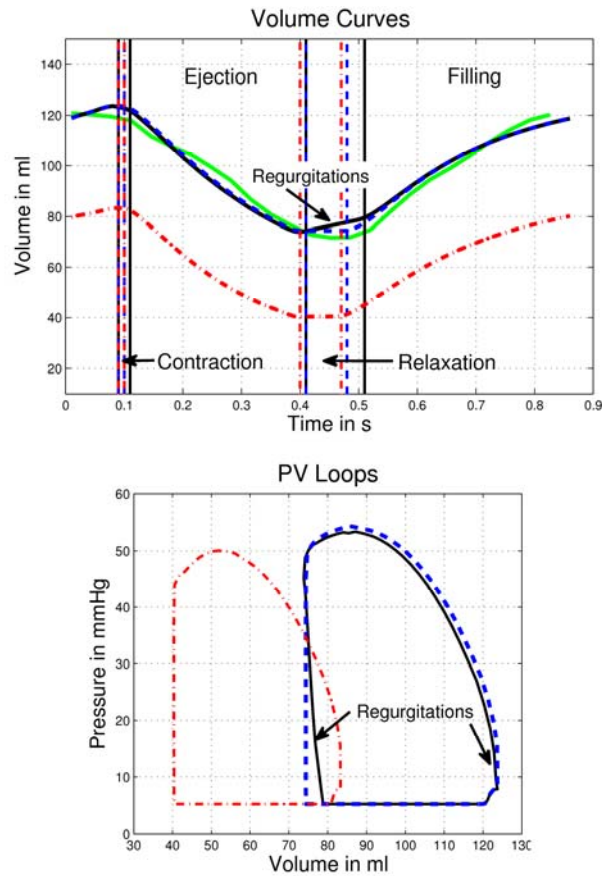


Fig. 6. RV volume curves and pressure-volume loops: (solid green) from segmentation; (solid black) preoperative simulation; (dashed blue) simulation after PPVR; (dash-dotted red) simulation after PVR with volume reduction. Vertical bars delineate the simulated cardiac phases. Regurgitations are visible during the isovolumetric phases, when volume should stay constant. As expected, RV volume reduction resulted in a shift of the curves.

Anatomical Model

Visual assessment of the dynamic segmentation showed good agreement (Fig. 3) despite the extremely dilated RV outflow tract. Table 1 provides the ejection fractions (EF) computed from the segmentation. These values will be used as reference when calibrating the EM model. RV volume curve is illustrated in Fig. 7 (green curve). The tetrahedral 3D model used for the simulation was made up of 65181 elements and the dyskinetic region identified on the images was manually delineated (Fig. 8a). To improve the numerical stability of the simulation, the myocardium was artificially thickened by dilating the epicardium.

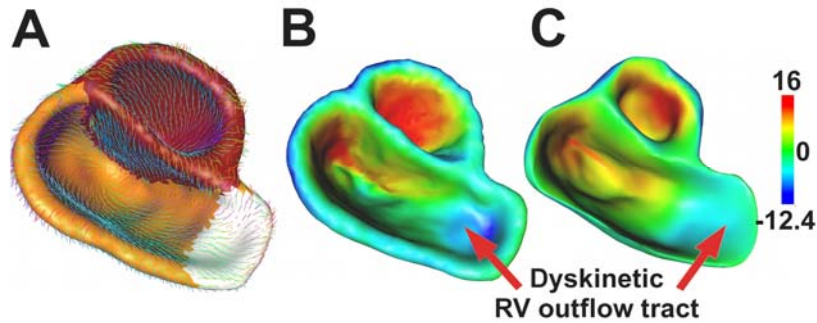


Fig. 7. a) 3D anatomical model at mid-diastole: (red) LV, (orange) RV, (white) observed dyskinetic area, (colour lines) fibre orientations. b-c) Radial displacements (in mm) between end-diastole and end-systole (positive values along the outer normal): b) end-systolic shape computed using the model c) end-systolic shape extracted from the images. Similar colour patterns between b) and c) confirm that the simulated model b) was able to exhibit in this patient realistic motion patterns, in particular the dyskinetic outflow tract.

EM Model Adjustment

Electrophysiology

Since there was no visible anomaly in electrophysiology, electrophysiology parameters were set as in a healthy heart ($v = 500 \text{ ms}^{-1}$, $\rho = 3$). Simulation and observations were time synchronised using the beginning of RV systole. Table 2 reports the computation time of the electrophysiology simulation, without biomechanics.

Biomechanics

Passive biomechanical properties were set according to values reported in the literature: Poisson ratio was set to ensure near-incompressibility of the myocardium ($\nu = 0.48$) and the ratio between fibre stiffness and cross-fibre stiffness was set to 3. Active biomechanical properties were manually personalised to the patient cardiac function. This was possible since a full cycle simulation only took about 15 minutes on a 2.4GHz Intel Core 2 Duo computer with 4GB of memory (Table 2). Finally, regurgitation flows ϕ_c and ϕ_r were estimated from the Doppler data ($\phi_c = \phi_r \approx 50 \text{ ml.s}^{-1}$).

Manual personalisation was performed as follows. We first started with reported values for healthy hearts ($\sigma_0 = 100 \text{ kPa.mm}^{-2}$; $\alpha_c = 10\text{s}^{-1}$; $\alpha_r = 20\text{s}^{-1}$). Then, the contractile element of the dyskinetic area was disabled to reproduce the abnormal motion of this region and, through a trial-and-error strategy, we manually adjusted the parameters for both ventricles to simulate the observed cardiac function. The manual adjustment was iteratively performed until the resulting simulated cardiac motion qualitatively coincided with the cine-MR images. The final parameters were: $\sigma_{0_{LV}} = 100 \text{ kPa.mm}^{-2}$; $\sigma_{0_{RV}} = 70 \text{ kPa.mm}^{-2}$; $\sigma_{0_{dysk}} = 0 \text{ kPa.mm}^{-2}$; $\alpha_c = 10\text{s}^{-1}$; $\alpha_r = 10\text{s}^{-1}$. We thus found a normal LV function whereas the RV contractility was weaker, probably because of its dilated morphology and possible fibrosis.

Preoperative Simulation

Realistic EF (Table 1), volume variations (Fig. 7, black solid curves) and RV systolic pressures ($\approx 54 \text{ mmHg}$) were obtained. Simulated normal displacements of the mesh vertices from their mid-diastole position were locally consistent with those computed from the segmentation (Fig. 8b-c). In particular, the simulated motions of the dyskinetic area, the RV septum and the LV were similar to those estimated from the segmentation. This confirms that the EM model was effectively calibrated and provided, for this patient, realistic motion patterns. Finally, despite our simple regurgitation model, the simulated pressure-volume (PV) loop was consistent with measurements in ToF reported in the literature [17] (this data was not available for this patient).

Table 1. Ejection fractions (EF) computed from the segmentation and simulations.

	LVEF	RVEF
Segmentation	61%	41%
Simulation: Preoperative	59%	40%
Simulation: PPVR	59%	40%
Simulation: PVR with RV Reduction	63%	51%

Percutaneous PVR Simulation

As mentioned in the introduction, PPVR consists in replacing the pulmonary valves using a minimally invasive procedure. The unique change in the cardiac function just after the intervention is thus the stopping of the pulmonary regurgitations. Hence, PPVR therapy was simulated by disabling the regurgitations in our model. After PPVR, the myocardium efficiency was improved: simulated isovolumetric phases were shorter and the end-systolic pressure higher (Fig. 7, dashed curves). However, no significant improvement in the pump function was obtained (Table 1). One possible reason could be that our limited regurgitation model accounts for regurgitations that occur during the isovolumetric phases only. Regurgitated volumes during the other phases may have an impact on the preoperative EF.

Simulation of PVR with RV Volume Reduction

As for PPVR, valve replacement was simulated by disabling the regurgitations. Virtual RV volume reduction was performed as illustrated in Fig. 9. First, the observed dyskinetic area (Fig. 8a) was resected in 3 steps. As reported in Table 2, interactivity was ensured despite the important number of tetrahedra that were removed. Then, the user interactively closes the free-wall. The framerate of the whole process was about 3 fps. Finally, the postoperative scar was simulated by setting the local conduction velocity v near the surgical junction to 0 ms^{-1} .

Table 2. Computation time. Values are obtained with a 2.4GHz Intel Core 2 Duo, 4GB of memory.

Electromechanical Simulation of the Heart	
1 heart beat, electrophysiology	≈ 1 minute
1 heart beat, electromechanics	≈ 15 minutes
Virtual Surgery	
Framerate	3 fps
Resection, step 1/3 (3938 elements)	0.73s
Resection, step 2/3 (966 elements)	0.08s
Resection, step 3/3 (1404 elements)	0.12s

After the virtual intervention, RV volume effectively decreased (Fig. 7, dash-dotted curves) and RV postoperative EF improved significantly (Table 1). Observe that LV EF also increased, which highlights the close relationship between LV and RV function. Finally, RV systolic pressure slightly decreased mainly because of the scar (non reported simulations without the scar resulted in unchanged RV systolic pressure).

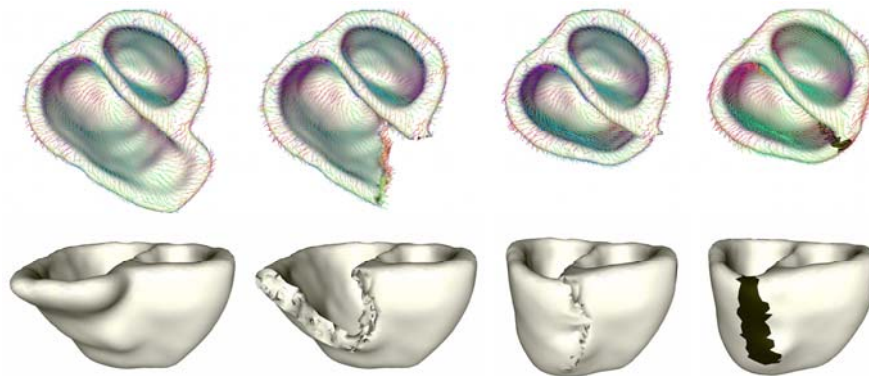


Fig. 8. Virtual RV volume reduction surgery. From left to right: original mesh, after resection, during attachment, final mesh. Colour lines: fibre orientations. Black area: postoperative scar.

Discussion

We have studied the potential of image processing techniques, EM models and virtual soft-tissue intervention platforms to perform virtual and personalised as-

assessment of PVR therapies. The results were promising and suggested that such tools might be used by the clinicians to test different PVR therapies.

A modular framework has been proposed. A simplified but fast EM model was adjusted to the purposes of the study and an interactive soft-tissue intervention platform was adapted. Still, the framework managed to realistically simulate the cardiac function of a randomly selected patient with repaired ToF. For this patient, we found that PVR with RV volume reduction would yield better results than PPVR, just after the intervention. Probable reasons may be the removal of the dysknetic area and the direct reduction of the RV volume. However, this procedure is very invasive and may be hazardous for the patient, with possible postoperative side effects such as electrophysiological troubles due to the surgical scar. On the other hand, it is worth mentioning that the effects of PPVR are often visible late after replacement. The myocardium adapts itself to its new loading conditions. We thus need to model this phenomenon to simulate the long-term postoperative effects of PPVR.

Based on these observations and owing to the modularity of our framework, more complex models can be used. In particular, future works include improvements of the regurgitation model, to take into account the other compartments, simulation of the long-term effects of the PVR therapies, by considering myocardium remodelling, automated estimation of biomechanical parameters and comprehensive validation using preoperative and postoperative clinical data.

Acknowledgments The work has been partly funded by the European Commission through the IST-2004-027749 Health-e-Child Integrated Project (<http://www.health-e-child.org>)

References

1. CGAL. <http://www.cgal.org>
2. GHS3D. <http://www-c.inria.fr/gamma/ghs3d/ghs.php>
3. SOFA. <http://www.sofa-framework.org>
4. Allard J, Cotin S, Faure F, Bensoussan PJ, Poyer F, Duriez C, Delingette H, Grisoni L (2007) SOFA – An Open Source Framework for Medical Simulation. In: *Medicine Meets Virtual Reality (MMVR'15)*
5. André B, Delingette H (2008) Versatile design of changing mesh topologies for surgery simulation. In: *International Symposium on Computational Models for Biomedical Simulation - (ISBMS08)*
6. Arts T, Costa KD, Covell JW, McCulloch AD (2001) Relating myocardial laminar architecture to shear strain and muscle fiber orientation. *Am J Physiol Heart Circ Physiol* **280**(5):2222–2229
7. Bestel J, Clément F, Sorine M (2001) A biomechanical model of muscle contraction. In: *Proc. MICCAI 2001*, pp. 1159–1161
8. Hunter PJ, Pullan AJ, Smaill BH (2003) Modeling total heart function. *Annu Rev Biomed Eng* **5**:147–177
9. Kaus MR, von Berg J, Weese J, Niessen W, Pekar V (2004) Automated segmentation of the left ventricle in cardiac MRI. *Med Image Anal* **8**(3):245–254

16 Tommaso Mansi , Barbara André , Michael Lynch , Maxime Sermesant , Hervé Delingette , Younes Boudjemline and Nicholas Ayache

10. Keener J, Sneyd J (1998) *Mathematical physiology*. Springer-Verlag
11. Khambadkone S, Coats L, Taylor A, Boudjemline Y, Derrick G, Tsang V, Cooper J, Muthurangu V, Hegde SR, Razavi RS, Pellerin D, Deanfield J, Bonhoeffer P (2005) Percutaneous pulmonary valve implantation in humans: Results in 59 consecutive patients. *Circulation* 112(8):1189–1197
12. Lorenzo-Valdes M, Sanchez-Ortiz GI, Elkington AG, Mohiaddin RH, Rueckert D (2004) Segmentation of 4D cardiac MR images using a probabilistic atlas and the EM algorithm. *Medical Image Analysis* 8(3):255–265
13. McCulloch A, Bassingthwaite J, Hunter P, Noble D (1998) Computational biology of the heart: from structure to function. *Prog Biophys Mol Biol* 69(2-3)
14. Montagnat J, Delingette H (2005) 4D deformable models with temporal constraints: application to 4D cardiac image segmentation. *Med Image Anal* 9(1):87–100
15. Nesme M, Payan Y, Faure F (2005) Efficient, physically plausible finite elements. In: J. Dingliana, F. Ganovelli (eds.) *Eurographics* (short papers)
16. del Nido PJ (2006) Surgical management of right ventricular dysfunction late after repair of tetralogy of Fallot: Right ventricular remodeling surgery. *Semin Thorac Cardiovasc Surg Pediatr Card Surg Annu.* 9(1):29–34
17. Redington AN, Rigby ML, Shinebourne EA, Oldershaw PJ (1990) Changes in the pressure-volume relation of the right ventricle when its loading conditions are modified. *Br. Heart J.* 63(1):45–49
18. Sermesant M, Delingette H, Ayache N (2006) An electromechanical model of the heart for image analysis and simulation. *IEEE TMI* 25(5):612–625
19. Sermesant M, Konukoglu E, Delingette H, Coudière Y, Chinchapatnam P, Rhode K, Razavi R, Ayache N (2007) An anisotropic multi-front fast marching method for real-time simulation of cardiac electrophysiology. In: *Proc. FIMH 2007*, pp. 160–169
20. Stergiopoulos N, Westerhof BE, Westerhof N (1999) Total arterial inertance as the fourth element of the windkessel model. *Am J Phys Heart Circ Phys* 276(1)
21. Tang D, Yang C, Geva, T, del Nido PJ (2007) Patient-specific virtual surgery for right ventricle volume reduction and patch design using MRI-based 3D FSI RV/LV/patch models. In: *Proc. CME 2007*, pp. 157–162
22. Turk G, O’Brien J (1999) Variational implicit surfaces. Tech. rep., Georgia Institute of Technology (1999)
23. Vercauteren T, Pennec X, Perchant A, Ayache N (2007) Non-parametric diffeomorphic image registration with the demons algorithm. In: *Proc. MICCAI 2007*
24. Wong KCL, Wang L, Zhang H, Liu H, Shi P (2007) Integrating functional and structural images for simultaneous cardiac segmentation and deformation recovery. In: *Proc. MICCAI 2007*, vol. 4791, pp. 270–277, Springer Berlin / Heidelberg
25. Zheng Y, Barbu A, Georgescu B, Scheuering M, Comaniciu D (2007) Fast automatic heart chamber segmentation from 3D CT data using marginal space learning and steerable features. In: *Proc. ICCV 2007*, pp. 1–8